Supporting Information

Site-Specific Immuno-PET Tracer to Image PD-L1

Haley L. Wissler[1,†], Emily B. Ehlerding[2,†], Zhigang Lyu[1], Yue Zhao[1], Si Zhang[1], Anisa Eshraghi[1], Zakey Yusuf Buuh[1], Jeffrey C. McGuth[1], Yifu Guan[1], Jonathan W. Engle[2], Sarah J. Bartlett[1], Vincent A. Voelz[1], Weibo Cai[2,*], Rongsheng E. Wang[1,*]

1. *Department of Chemistry, Temple University, 1901 N. 13th Street, Philadelphia, PA, 19122, USA*

2. *Departments of Radiology and Medical Physics, University of Wisconsin-Madison, WI, 53705, USA*

* To whom correspondence should be addressed:

Weibo Cai, Phone (608) 262-1749. Email: wcai@uwhealth.org

Rongsheng E. Wang, Phone (215) 204-1855. Email: rosswang@temple.edu

† These authors contributed equally.

Table of Contents

Experimental Methods:

Chemical synthesis

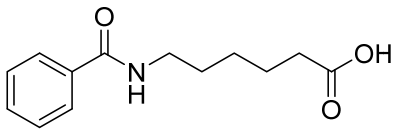

1

6-Benzoylamino-hexanoic acid (compound **1**) was synthesized following the published procedure.[1] ^{1}H NMR (500MHz, $CDCl_3$): δ 1.42(q, 2H), 1.59-1.70(m, 4H), 2.34(t, J=7.35 Hz, 2H), 3.45(q, J=6.0 Hz, 2H), 6.4(bs, 1H), 7.4(t, 2H), 7.48(m, 1H), 7.75(m, 2H); ^{13}C NMR (125 MHz, $CDCl_3$): δ 178.8, 167.9, 134.6, 131.4, 128.6, 126.9, 39.8, 33.8, 29.2, 26.3, 24.3. ESI-MS calculated for $C_{13}H_{17}NO_3$ $[MH]^+$ 236.3, observed 236.1.

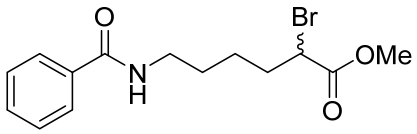

2

A mixture of compound **1** (3 g, 0.0128 mol) and dry red phosphorus (0.53 g, 0.0172 mol) were cooled down by an ice-salt bath. After dropwise addition of bromine (8.16 g, 0.102 mol), the ice bath was removed and the mixture was refluxed overnight at ~ 100 ºC. The reaction mixture was cooled to room temperature and then 0 ºC, followed by dropwise addition of 20 mL of methanol. After another reflux at 100 ºC for 30 min, the mixture was promptly concentrated and dissolved in 100 mL of ethyl acetate, washed with saturated sodium bicarbonate, saturated sodium thiosulfate, and eventually brine. The organic phase was concentrated to a crude oil and purified via flash chromatography (5:1, Hexane: Ethyl Acetate) to render pure compound **2** at an 85% yield (3.57 g). ^{1}H NMR (500MHz, $CDCl_3$): δ 1.38(m, 1H), 1.51 (m, 1H), 1.61 (m, 2H), 2.0 (m, 2H), 3.4 (q, J=6.7 2H), 3.7 (s, 3H), 4.2 (t, J=7.39, 1H), 7.4(t, 2H), 7.48(m, 1H), 7.75(m, 2H); ^{13}C NMR (125 MHz, $CDCl_3$): δ 170.3, 167.8, 134.6, 131.3, 128.4, 127.0, 53.0, 45.5, 39.6, 34.3, 28.7, 24.6.

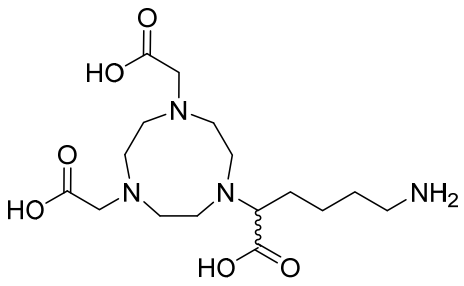

3

The coupling of linker **2** towards NOTA compound follows the published procedures[1, 2] with modifications. Briefly, 72.6 mg (0.203 mmol) 1,4,7-Triazacyclononane-1,4-bis(t-butyl acetate) (Macrocyclics, Inc) was mixed with 82.3 mg compound **2** (0.243 mmol), and 33.6 mg K_2CO_3 (0.243 mmol) in 5 mL dry acetonitrile under nitrogen protection. The reaction mixture was refluxed for 48 h, and then concentrated after the completion of the reaction as confirmed by TLC. The crude was re-dissolved in 4 mL of 6 M aqueous HCl and refluxed for 24 h. The hydrolyzed product was purified via HPLC to yield compound **3** in ~ 50% yield (38 mg) over two steps. ^{1}H NMR (500MHz, D_2O): δ 1.45 (m, 2H), 1.65 (m, 2H), 1.75 (m, 1H), 1.87 (m, 1H), 2.95 (t, 2H), 3.2 (m, 12H), 3.6 (t, 1H), 3.9 (s, 4H); ^{13}C NMR (125 MHz, D_2O): δ 175.3, 172.2, 64.8, 55.4, 50.5, 46.3, 39.1, 27.8, 26.6, 23.1. ESI-MS calculated for $C_{16}H_{30}N_4O_6$ $[MH]^+$ 375.2, observed 375.2.

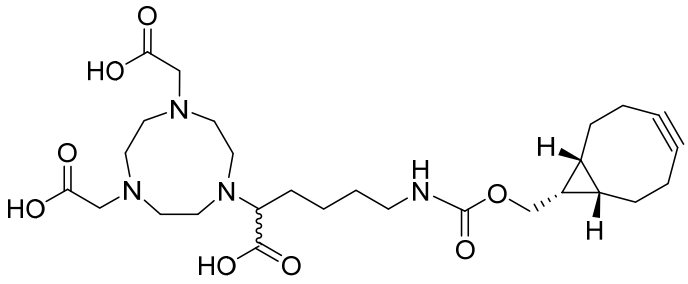

4

To a flame-dried flask, 6.9 mg compound **3** (0.0185 mmol) and 5.4 mg (0.0185 mmol) BCN-succinimidyl ester (Sigma Aldrich) were added and dissolved in anhydrous DMF. After the addition of n-methylmorpholine (3.75 mg, 0.037mmol), the reaction mixture was stirred for 4h, and monitored via LC-MS for a full conversion of the succinimidyl ester. After vacuum concentration, the final mixture was purified by HPLC to afford 3.2 mg compound **4** as a pale white solid (~ 31% yield). ^{1}H NMR (500MHz, D_2O): δ 0.80 (m, 2H), 1.15 (m, 2H), 1.4-1.6 (m, 6H), 1.7-2.0 (m, 6H), 2.15-2.35 (m, 2H), 2.5-2.75 (m, 2H), 3.1 (s, 12H), 3.6 (bs, 1H), 3.8 (s, 4H), 4.15 (m, 2H); . ^{13}C NMR (125 MHz, D2O): δ 179.2, 177.1, 175.7, 100.3, 67.2, 63.6, 57.3, 56.9, 50.5, 50.1, 49.4, 48.1, 47.7, 44.7, 40.2, 29.3, 28.8, 28.5, 23.2, 20.7, 19.7, 17.2. HRMS calculated for $C_{27}H_{43}N_4O_8$ $[MH]^+$ 551.3081, observed 551.3055.

Cloning of antibody expression vectors

The gene fragments encoding the Fab fragments of αPD-L1 and αHer2 (trastuzumab) were synthesized by Integrated DNA Technologies (IDT), amplified by PCR, and cloned into the pBAD vector backbone (Thermo Fisher) through digestion and ligation with responsible enzymes (New England Biolabs). Unnatural amino acid incorporation was introduced onto the Fab fragments by mutating the desired site to the TAG amber nonsense codon with a Q5 site-directed mutagenesis kit (New England Biolabs).[3] Final vectors' sequences were confirmed by Sanger Sequencing (GENEWIZ).

Antibody sequences

Anti-PD-L1 Fab light chain:

QSALTQPASVSGSPGQSITISCTGTSSDVGGYNYVSWYQQHPGKAPKLMIYDVSNRPSG
VSNRFSGSKSGNTASLTISGLQAEDEADYYCSSYTSSSTRVFGTGTKVTVLGQPKANPTV
TLFPPSSEELQANKATLVCLISDFYPGAVTVAWKADGSPVKAGVETTKPSKQSNNKYAA
SSYLSLTPEQWKSHRSYSCQVTHEGSTVEKTVAPTECS

Anti-PD-L1 Fab heavy chain:

EVQLLESGGGLVQPGGSLRLSCAASGFTFSSYIMMWVRQAPGKGLEWVSSIYPSGGITF
YADTVKGRFTISRDNSKNTLYLQMNSLRAEDTAVYYCARIKLGTVTTVNYWGQGTLVT
VSSASTKGPSVFPLAPSSKSTSGGTAALGCLVKDYFPEPVTVSWNSGALTSGVHTFPAVL
QSSGLYSLSSVVTVPSSSLGTQTYICNVNHKPSNTKVDKKVEPKSCDKTHT

Anti-Her2 trastuzumab Fab light chain:

DIQMTQSPSSLSASVGDRVTITCRASQDVNTAVAWYQQKPGKAPKLLIYSASFLYSGVP
SRFSGSRSGTDFTLTISSLQPEDFATYYCQQHYTTPPTFGQGTKLEIKRTVAAPSVFIFPPS
DEQLKSGTASVVCLLNNFYPREAKVQWKVDNALQSGNSQESVTEQDSKDSTYSLSSTL
TLSKADYEKHKVYACEVTHQGLSSPVTKSFNRGEC

Anti-Her2 trastuzumab Fab heavy chain:

EVQLVESGGGLVQPGGSLRLSCAASGFNIKDTYIHWVRQAPGKGLEWVARIYPTNGYT
RYADSVKGRFTISADTSKNTAYLQMNSLRAEDTAVYYCSRWGGDGFYAMDYWGQGT
LVTVSSASTKGPSVFPLAPSSKSTSGGTAALGCLVKDYFPEPVTVSWNSGALTSGVHTFP
AVLQSSGLYSLSSVVTVPSSSLGTQTYICNVNHKPSNTKVDKKVEPKSCDKTHT

Expression and purification of antibody Fab fragments

For expression of wt antibodies, 8 mL 2YT medium was supplemented with 100 μg/mL ampicillin and inoculated with the E. coli stock carrying the desired pBAD plasmid. After overnight incubation at 37 °C, 250 rpm (MaxQ8000, Thermo Scientific), the culture was diluted into 800 mL ampicillin-containing 2YT medium and was continuously shaken at 37 °C, 250 rpm. Once the

OD_{600} reached 0.8, protein expression was induced by 0.2% arabinose, with subsequent shaking for 24h at 37 ^{o}C, 250 rpm (MaxQ8000, Thermo Scientific). To extract desired proteins, cells were then harvested and lysed in 80 mL periplasmic lysis buffer (20% sucrose, 30 mM Tris (pH 8.0), 1 mM EDTA, and 0.2 mg/mL lysozyme). Cell lysates were centrifuged (9000 rpm for 40 min, Allegra, Beckman Coulter) to remove the debris, and passed through a 0.22 μm filter for sterilization. The Fab proteins were enriched and purified by passing the filtered lysates through a CH1 affinity column (Capture Select, Thermo Fisher), and were eventually eluted out with an elution buffer (100 mM glycine, pH 2.8), followed by immediate neutralization with 1M Tris buffer. After rounds of buffer exchange with Amicon filters (Sigma Aldrich), the desired proteins were stored in PBS buffer, pH 7.4. Their identities and purities were characterized by SDS-PAGE and ESI-MS.

For expression of the Fab mutants containing unnatural amino acids, procedures were similar to those above except that the pULTRA-pAzF (encodes orthogonal *Methanocaldococcus jannaschii* tRNA and aminoacyl-tRNA synthetase for para-azido phenylanaline (pAzF)) vector was co-transformed with the pBAD vector. In addition to 100 μg/mL ampicillin, all media were supplemented with 100 μg/mL spectinomycin to ensure the carrying of pULTRA vector. At the inoculation stage, 1 mM pAzF was added into the expression media. When OD_{600} reached 0.8, 1 mM IPTG was added in addition to arabinose to induce necessary protein expression from both vectors.

In silico screening of mutation sites on αPD-L1 Fab

The RosettaBackrub algorithm was used to predict changes in the fold stability of αPD-L1 upon single point mutations.[4] This algorithm is based on structural modeling of protein conformations, taking into account backbone flexibility during Monte Carlo sampling.[5] Since the algorithm has not been parameterized for non-canonical amino acids like pAzF, we considered mutations to alanine and phenylalanine as useful proxies.

For each of the 23 proposed mutations, the RosettaBackrub algorithm outputs twenty structural models and their corresponding scores in Rosetta Energy Units (REU). REUs are an energy-like quantity, with lower scores predicting greater stability, which we compare to the wild-type model to rank the resulting predictions. The score reported by the RosettaBackrub algorithm is the default Rosetta full-atom energy function and weight set, which is internally referred to as *score12*. While Rosetta scores cannot be directly used in place of mutational $\Delta\Delta G$ values, correlations can be inferred from the terms in the Rosetta energy function.[6]

Predictions of the RosettaBackrub algorithm for the 23 proposed mutations are shown in Figure 2A. Similar changes in stability are predicted for alanine and phenylalanine (Figure 2B). Mutations at HC_K129 are predicted to be the most favorable of the 23 selected residues, while mutations at LC_V202, in contrast, are not ranked as especially favorable (Figure 2C).

Site-specific conjugation and purification of Fab-NOTA conjugates

The BCN-NOTA linker described in supplementary scheme 1 is composed of a BCN unit allowing for copper-free [3+2] 'click' chemistry and a NOTA moiety to chelate radionuclides for PET imaging. For 'click'-based conjugation of the linker towards pAzF on the antibody mutant,[7] Fab mutants of αPD-L1 or αHer2 (0.45 mg, 9 nmol) were concentrated to 2.5 mg/mL (~ 50 μM) in PBS buffer. NOTA-BCN linker (0.05 mg, 90 nmol, ~ 500 μM) was added, and the reaction mixture was incubated at 37 °C for 12h to ensure the complete conjugation. The Fab conjugates were purified based on the reported procedure.[3, 8, 9] The purity and the extent of labeling were characterized by SDS-PAGE and ESI-qTOF high resolution MS.

ELISA assay of anti-PD-L1 Fab fragments and anti-PD-L1 Fab-NOTA conjugates

The ELISA assays of wild type αPD-L1 Fab fragment, αPD-L1 Fab mutant (HC-K129 pAzF), and the αPD-L1 Fab conjugate with NOTA-BCN linker were carried out in parallel for comparison. Briefly, a flat-bottom 96-well black plate (Maxisorp, Nunc) was coated with PD-L1 Fc chimera (R&D Systems), and blocked with 1% BSA. After washing the wells with PBS/0.05% Tween, the Fab fragments or the conjugation product were serially diluted in the blocking buffer (PBS, 1% BSA) and transferred into wells in triplicate at 100 μL/well. After 2h incubation and subsequent washing, HRP-labelled anti-human lambda light chain (Sigma Aldrich) was added and incubated for an additional 1 h. Immediately following extensive washing (5 times), 100 μL/well QuantaBlu fluorogenic ELISA substrate (Thermo Fisher) was added to all the wells. The fluorescence signals were detected and recorded by a Synergy H1 plate reader (BioTek). The data was further processed and plotted using GraphPad Prism (GraphPad Software).

Radiolabeling of anti-PD-L1 Fab-NOTA conjugates

The radiolabeling procedures were carried out similar to previously reported procedures.[10, 11] For radiolabeling the αPD-L1- and αHER2- NOTA conjugates, $^{64}CuCl_2$ was first diluted in 150 – 300 μL of sodium acetate buffer (pH~5). The antibody fragments and radionuclide were then incubated for 1 h at 37°C under constant shaking at a ratio of 50 μg protein to 1 mCi of ^{64}Cu. To purify the samples after radiolabeling, the solutions were passed through a PD-10 column (GE Healthcare) using phosphate buffered saline (PBS) as the mobile phase. Injectable solutions were prepared in sterile PBS.

***In vivo* PET Imaging**

Athymic nude mice (n=3 per group, Crl: NU(NCr)-Foxn1nu, Envigo) were intravenously injected with 50-70 μCi (1.85 – 2.6 MBq) of either ^{64}Cu-NOTA-αPD-L1 Fab conjugate or ^{64}Cu-NOTA-αHER2 Fab conjugate. Mice were anesthetized using 3%/1% induction/maintenance isoflurane inhalation. Serial PET scans were then acquired at 5, 15, and 45 minutes post-injection of the tracers using an Inveon microPET/CT scanner (Siemens). 20 million counts per mouse were obtained at each imaging timepoint, and a 3D ordered subsets expectation maximization reconstruction algorithm was employed. A blocking study was also conducted to verify the

specificity of the PD-L1 tracer by administering ~200 μg of αPD-L1 wild type Fab 30 min prior to injection of ^{64}Cu-NOTA-αPD-L1. PET scans were then performed as for the other groups.

Similar procedures were used for imaging of C57BL/6 mice (n=3 per group, Envigo). Mice were injected with 50-70 μCi (1.85 – 2.6 MBq) of ^{64}Cu-NOTA-αPD-L1 Fab conjugate or ^{64}Cu-NOTA-αHer2 Fab conjugate and PET scans were completed at 5, 15, 45, and 90 min post-injection.

Quantitative data was extracted from PET images using the Inveon Research Workspace software to draw regions-of-interest (ROI). The accumulation of Fab conjugates in the tissues of interest was reported in %ID / gram, following the equation as shown below:

%ID/g = [activity in tissue (uCi/gram) / administered activity (uCi)] x100%

At the end of the terminal imaging scan, mice were euthanized through CO_2 asphyxiation and several organs and tissues were extracted, wet-weighed, and their radioactive contents were assayed using an automated gamma counter (PerkinElmer). Data from these biodistribution studies are also presented as %ID/g.

Immunofluorescence staining

Organs of significant uptake, including the spleen and brown adipose tissue, were excised from mice at the end of the imaging study, embedded in Optimal Cutting Temperature Compound (Sakura), sliced at 10 μm, and mounted for immunofluorescent analysis. For brown fat staining, the human/mouse cross-reactive antibody atezolizumab (Genentech Oncology) was conjugated with Cy3 dye and used for visualization of PD-L1 expression using standard procedures.[10] Spleen tissues were stained with atezolizumab and mouse anti-mouse CD45 primary antibodies, and the staining was completed with DyLight 650 donkey-anti-human and AlexaFluor 488 goat anti-mouse secondaries. In both instances, staining was completed through coverslipping the slides with DAPI-containing hard mount (Vector Laboratories), and imaging was performed using the Nikon A1R confocal microscope.

Supporting Figures:

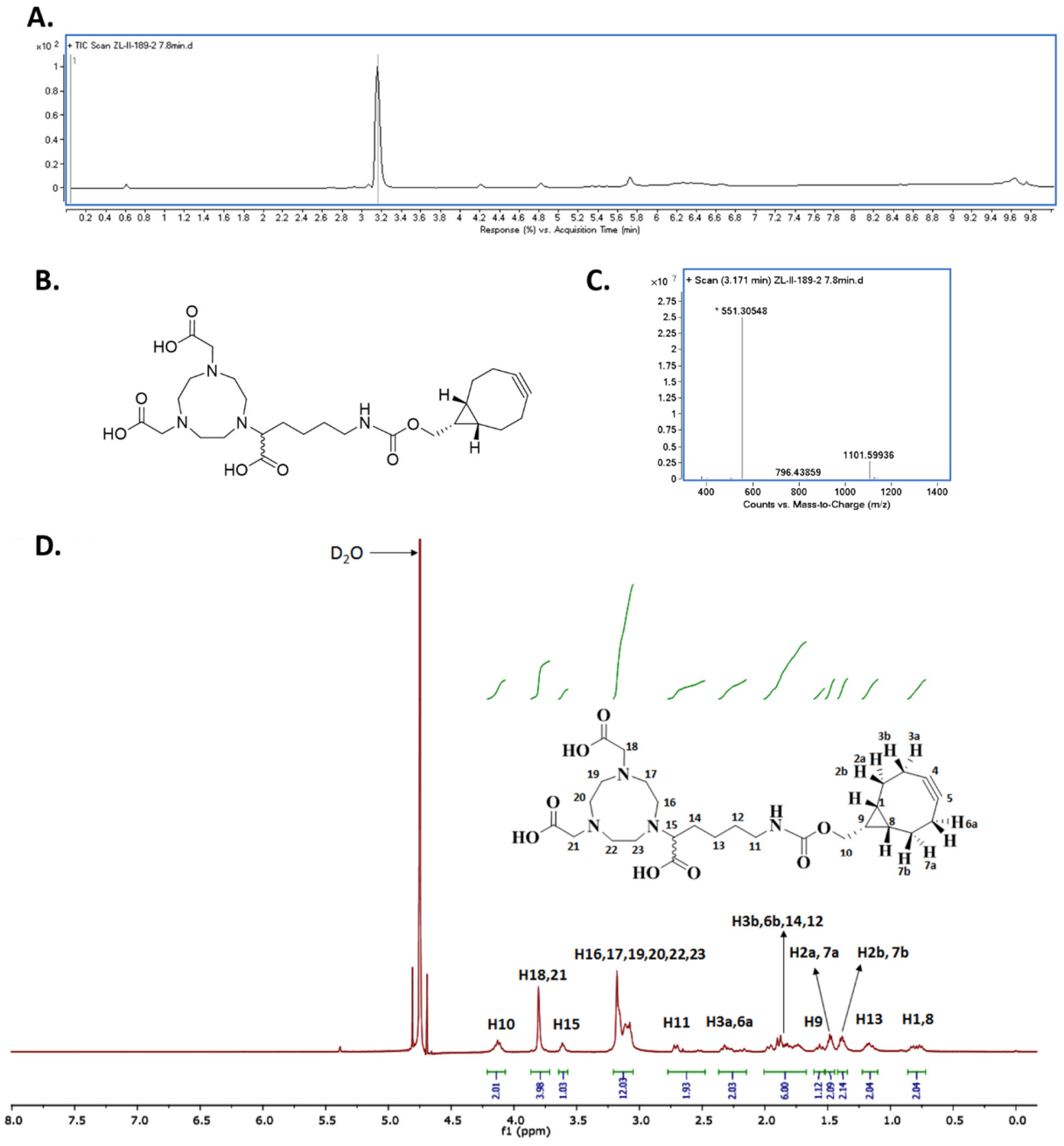

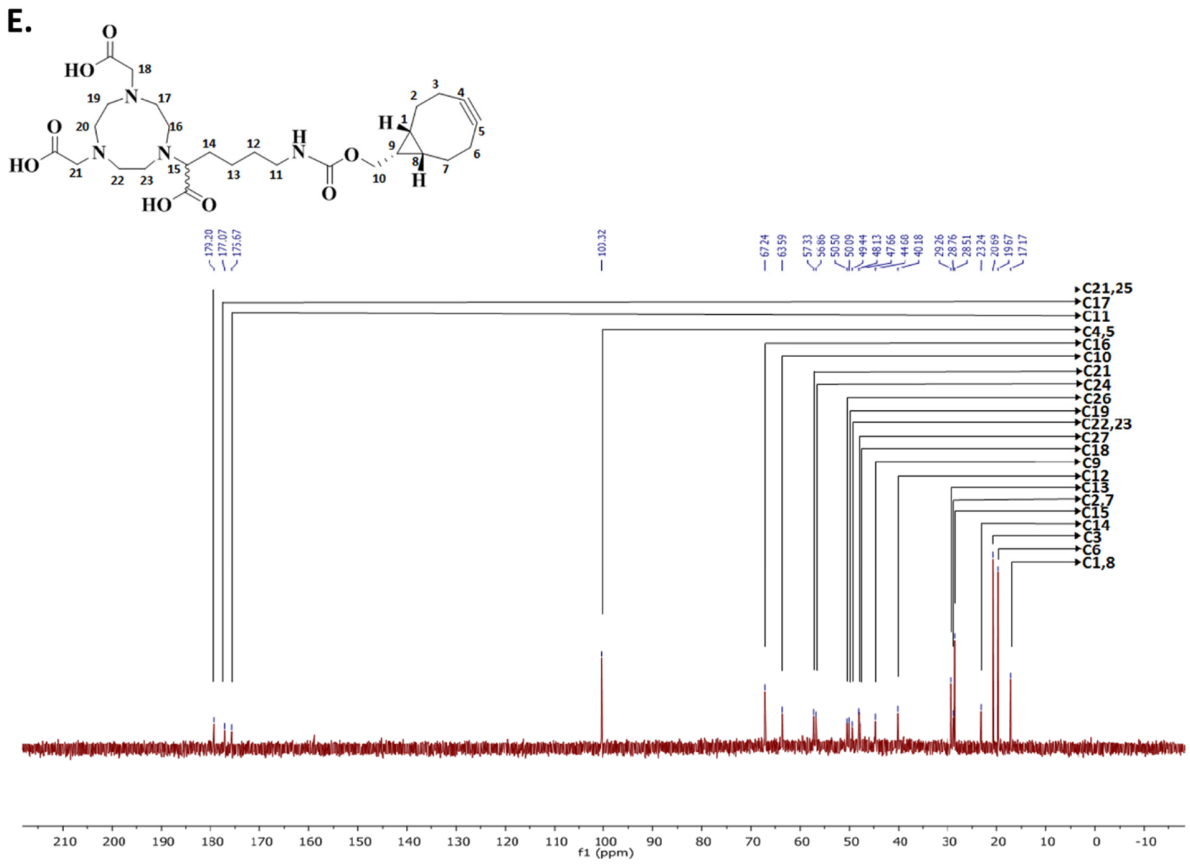

Figure S1. LC-MS and NMR analysis of compound 4, the NOTA-BCN linker. The flow rate was 1 mL/min. Solvent A was water/0.1% formic acid, and solvent B was acetonitrile/0.1% formic acid. Time 0 – 0.5 min, solvent B was 5%. Time 0.5 - 5.5 min, solvent B increased to 100%. Time 5.5 - 8.5 min, solvent B remained at 100%. Time 8.5 - 9 min, solvent B decreased to 5% and remained until the run stopped at 10min. (A) LC trace; (B) the chemical structure of NOTA-BCN; (C) high resolution MS scans; (D) the ^{1}H NMR spectrum; (E) the ^{13}C NMR spectrum.

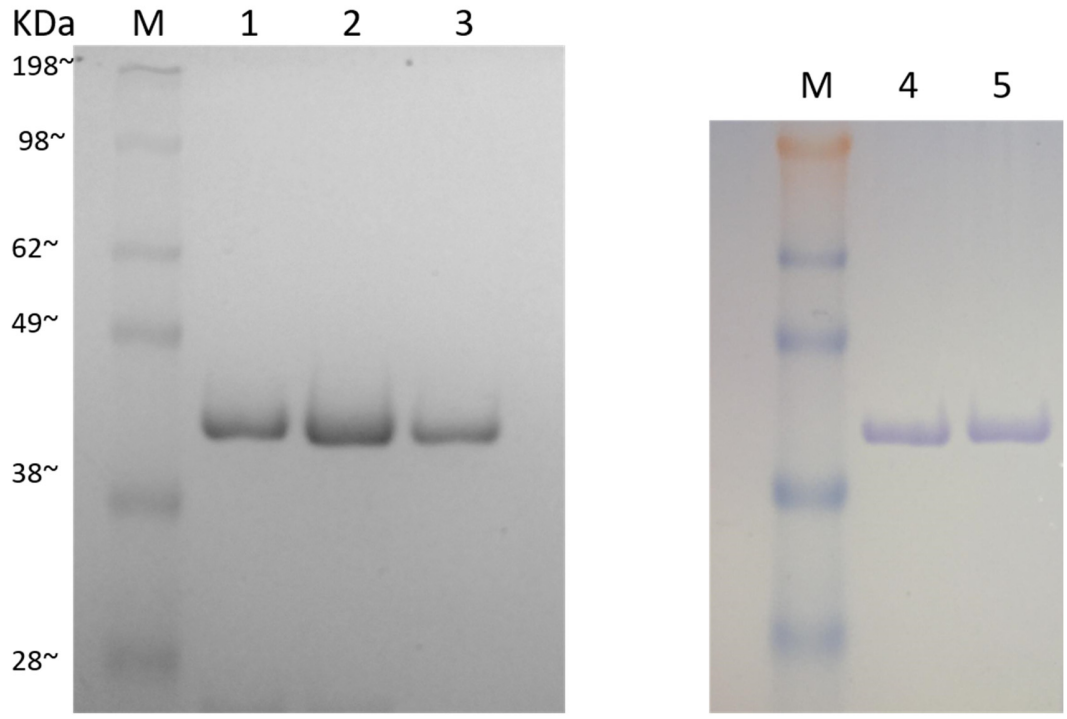

Figure S2. SDS-PAGE analysis of antibody Fab fragments. Lane 1: αPD-L1 Fab wild type; Lane 2: αPD-L1 Fab mutant (HC K129X, X = pAzF); Lane 3: Site-specific NOTA-αPD-L1 Fab conjugate (HC K129X, X = pAzF-BCN-NOTA); Lane 4: αHER2 Fab mutant (HC K129X, X = pAzF); Lane 5: Site-specific NOTA-αHER2 Fab conjugate (HC K129X, X = pAzF-BCN-NOTA).

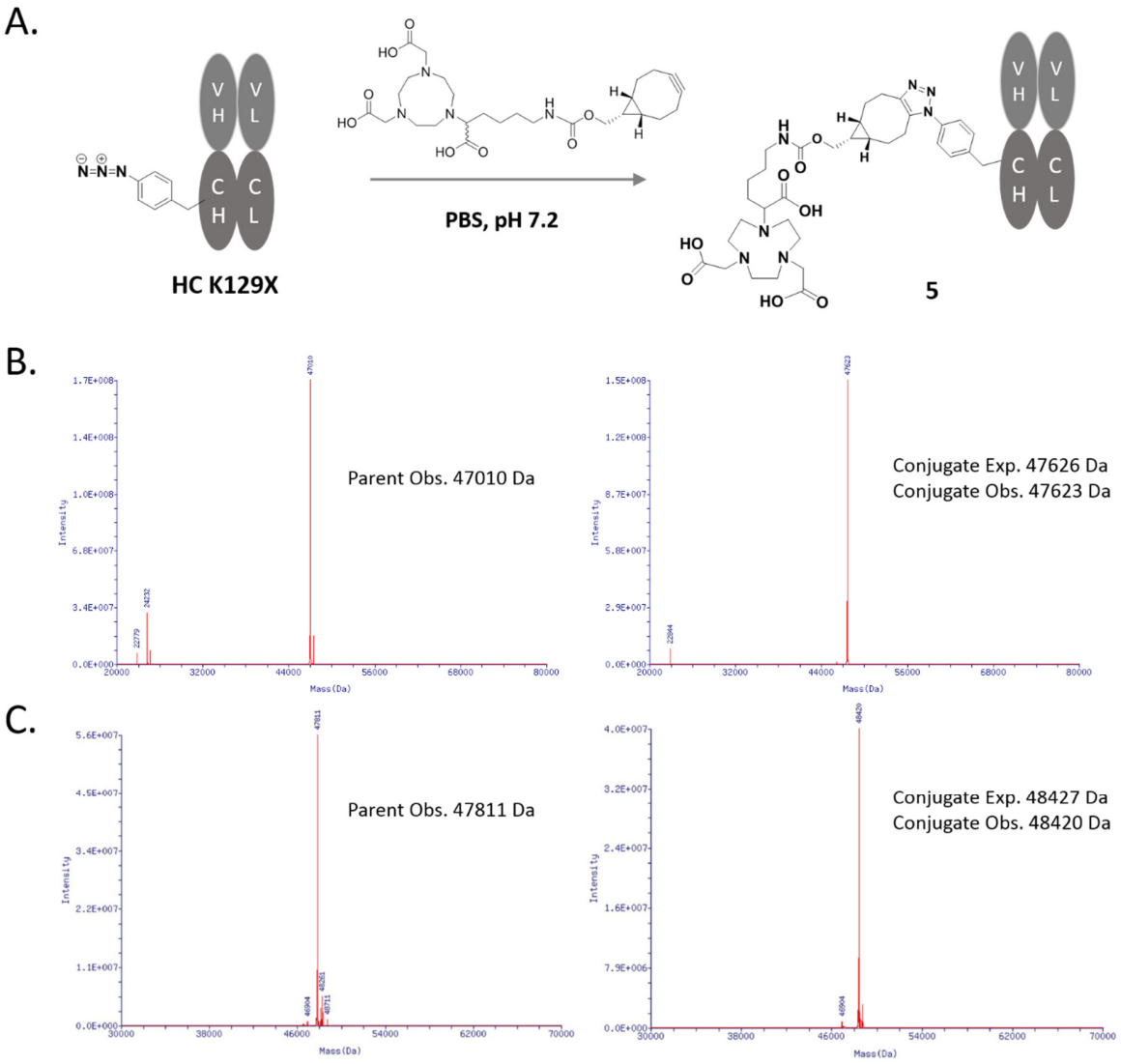

Figure S3. ESI-MS characterization of antibody conjugates with the BCN-NOTA linker. (A) Site-specific conjugation of the BCN-derivatized NOTA linker to antibody Fab fragment that incorporated pAzF at HC K129. (B) ESI-MS characterizations of the αPD-L1 Fab mutant before and after conjugation with one equivalent of BCN-NOTA. (C) ESI-MS characterizations of the αHER2 Fab mutant before and after conjugation with one equivalent of BCN-NOTA.

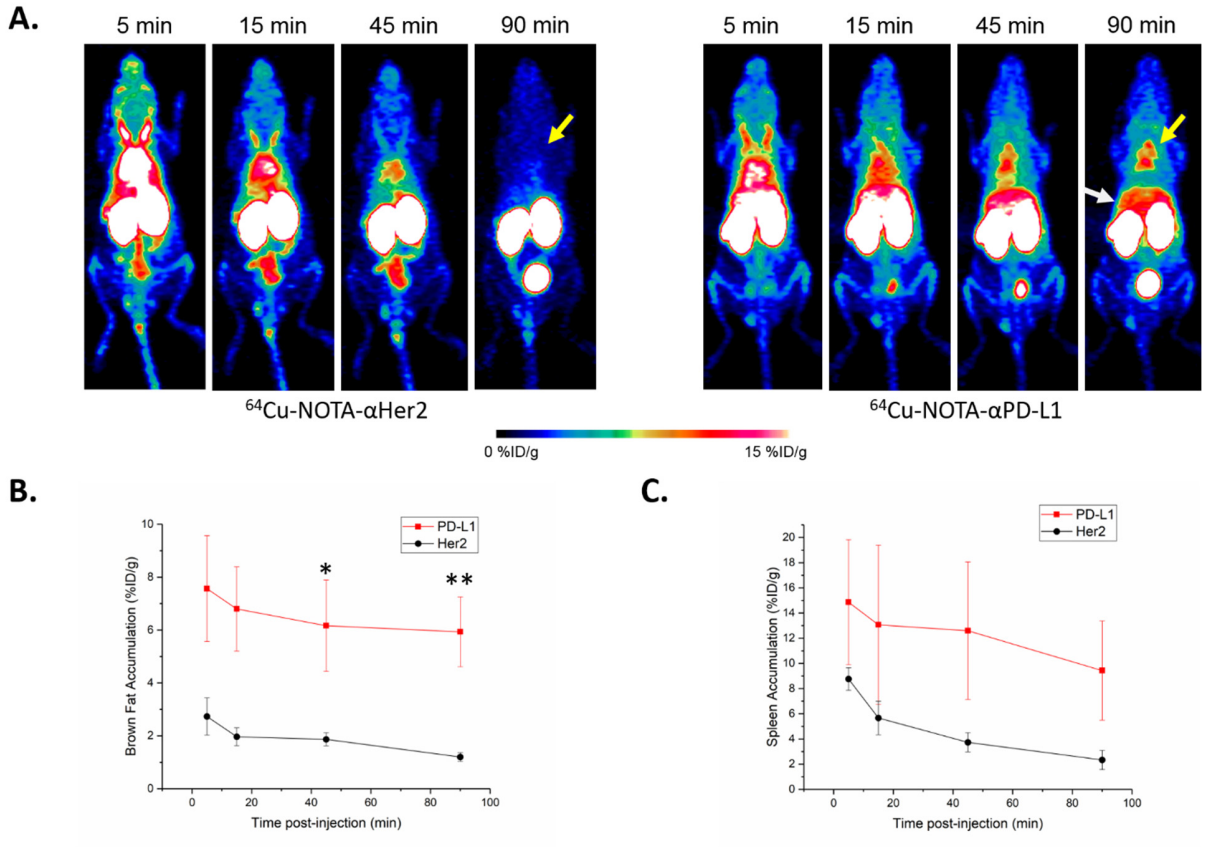

Figure S4. *In vivo* PET imaging studies with ^{64}Cu-NOTA-αPD-L1 and ^{64}Cu-NOTA-αHER2 in C57BL/6J mice. (A) PET scans at 5, 15, 45, and 90 min p.i. of either ^{64}Cu-NOTA-αHER2 (left) or ^{64}Cu-NOTA-αPD-L1 (right); yellow arrowhead indicates brown fat while white arrowhead points to the spleen. (B) Tracer uptake (%ID/g) in brown fat based on quantitative region-of-interest (ROI) analysis of the PET images. (C) Tracer uptake (%ID/g) in spleen. "*" represents $P < 0.05$; "**" represents $P < 0.01$. $n = 3$.

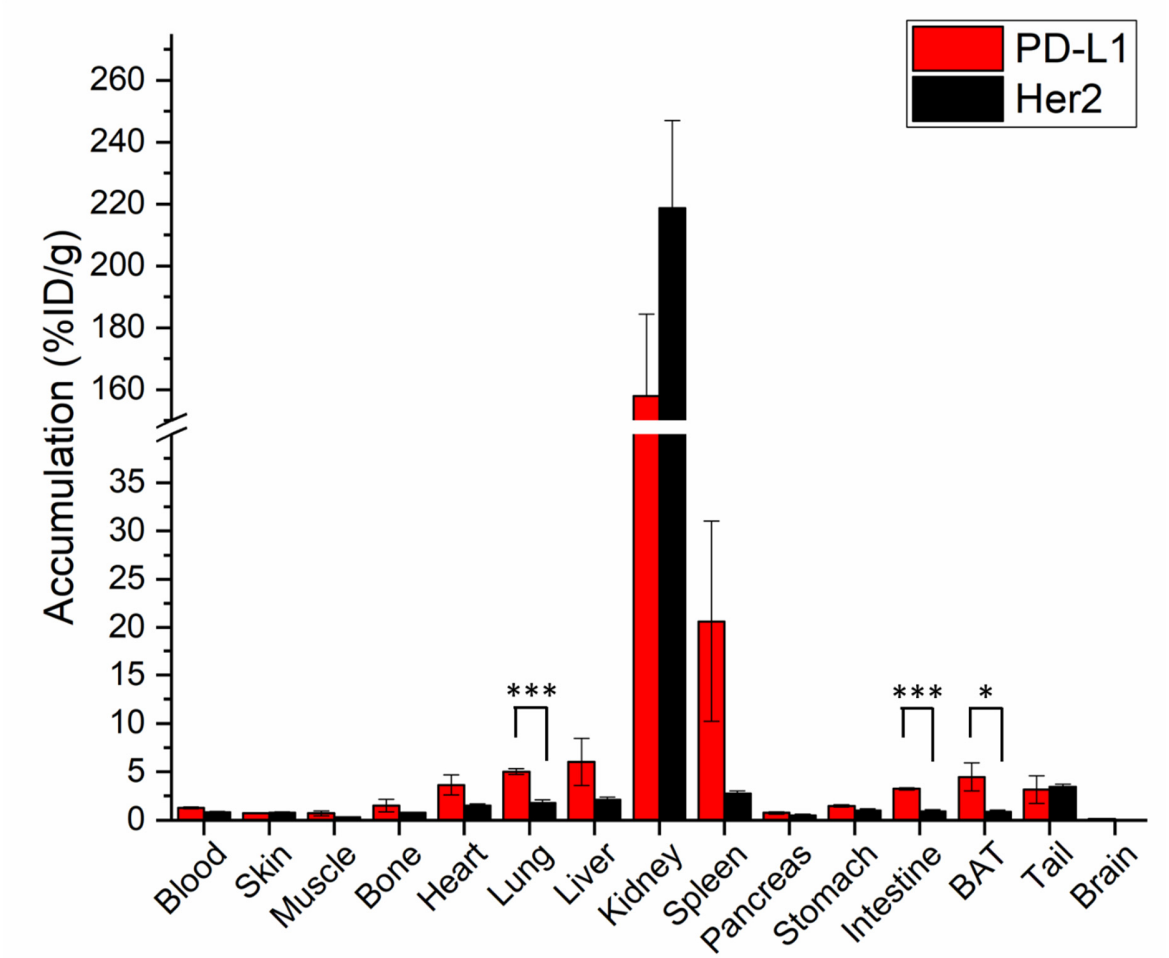

Figure S5. Ex vivo biodistribution of ^{64}Cu-NOTA-αPD-L1 and ^{64}Cu-NOTA-αHER2 in C57BL/6J mice at 90 min p.i. "*" represents $P < 0.05$; "***" represents $P < 0.001$. (n=3).

References

(1) Stasiuk, G. T., S; Imbert, D; Poillot, C; Giardiello, M; Tisseyre, C; Barbier, E; Henry Fries, P; de Waard, M; Reiss, P; Mazzanti, M. (2011) Cell-Permeable Ln(III) Chelate-Functionalized InP Quantum Dots As Multimodal Imaging Agents, *ACS Nano 5*, 8193-8201.

(2) Mate, G., Simecek, J., Pniok, M., Kertesz, I., Notni, J., Wester, H. J., Galuska, L., and Hermann, P. (2015) The influence of the combination of carboxylate and phosphinate pendant arms in 1,4,7-triazacyclononane-based chelators on their 68Ga labelling properties, *Molecules 20*, 13112-13126.

(3) Lyu, Z., Kang, L., Buuh, Z. Y., Jiang, D., McGuth, J. C., Du, J., Wissler, H. L., Cai, W., and Wang, R. E. (2018) A Switchable Site-Specific Antibody Conjugate, *ACS Chem. Biol. 13*, 958-964.

(4) Smith, C. A., and Kortemme, T. (2008) Backrub-Like Backbone Simulation Recapitulates Natural Protein Conformational Variability and Improves Mutant Side-Chain Prediction, *J. Mol. Biol. 380*, 742-756.

(5) Lauck, F., Smith, C. A., Friedland, G. F., Humphris, E. L., and Kortemme, T. (2010) RosettaBackrub--a web server for flexible backbone protein structure modeling and design, *Nucleic Acids Res. 38*, W569-W575.

(6) Kellogg, E. H., Leaver-Fay, A., and Baker, D. (2010) Role of conformational sampling in computing mutation-induced changes in protein structure and stability, *Proteins 79*, 830-838.

(7) Dommerholt, J., van Rooijen, O., Borrmann, A., Guerra, C. F., Bickelhaupt, F. M., and van Delft, F. L. (2014) Highly accelerated inverse electron-demand cycloaddition of electron-deficient azides with aliphatic cyclooctynes, *Nat. Commun. 5*, 5378.

(8) Wang, R. E., Liu, T., Wang, Y., Cao, Y., Du, J., Luo, X., Deshmukh, V., Kim, C. H., Lawson, B. R., Tremblay, M. S., Young, T. S., Kazane, S. A., Wang, F., and Schultz, P. G. (2015) An immunosuppressive antibody-drug conjugate, *J. Am. Chem. Soc. 137*, 3229-3232.

(9) Wang, R. E., Wang, Y., Zhang, Y., Gabrelow, C., Zhang, Y., Chi, V., Fu, Q., Luo, X., Wang, D., Joseph, S., Johnson, K., Chatterjee, A. K., Wright, T. M., Nguyen-Tran, V. T., Teijaro, J., Theofilopoulos, A. N., Schultz, P. G., and Wang, F. (2016) Rational design of a Kv1.3 channel-blocking antibody as a selective immunosuppressant, *Proc. Natl. Acad. Sci. U S A 113*, 11501-11506.

(10) Ehlerding, E. B., England, C. G., Majewski, R. L., Valdovinos, H. F., Jiang, D., Liu, G., McNeel, D. G., Nickles, R. J., and Cai, W. (2017) ImmunoPET Imaging of CTLA-4 Expression in Mouse Models of Non-small Cell Lung Cancer, *Mol. Pharm. 14*, 1782-1789.

(11) Ferreira, C. A., Hernandez, R., Yang, Y., Valdovinos, H. F., Engle, J. W., and Cai, W. (2018) ImmunoPET of CD146 in a Murine Hindlimb Ischemia Model, *Mol. Pharm. 15*, 3434-3441.